RESEARCH ARTICLE

Insight into the Folding and Cooperative Multi-Recognition Mechanism in Supramolecular Anion-Binding Catalysis

Dariusz G. Piekarski,*[a] Pascal Steinforth,[b] Melania Gómez-Martínez,[a] Julia Bamberger,[a] Florian Ostler,[a] Monika Schönhoff[b] and Olga García Mancheño*[a]

[a] Dr. D. G. Piekarski, Dr. M. Gómez-Martínez, Dr. J. Bamberger, F. Ostler, Prof. Dr. O. García Mancheño
Organic Chemistry Institute
University of Münster
Corrensstrasse 36, D-48149 Münster, Germany
E-mails: olga.garcia@uni-muenster.de; piekarsk@uni-muenster.de

[b] P. Steinforth, Prof. Dr. M. Schönhoff
Institute of Physical Chemistry
University of Münster
Corrensstrasse 28-30, D-48149 Münster, Germany

Supporting information for this article is given via a link at the end of the document.

Abstract: H-bond donor catalysts able to modulate the reactivity of ionic substrates for asymmetric reactions have gained great attention in the past years, leading to the development of cooperative multidentate H-bonding supramolecular structures. However, there is still a lack of understanding of the forces driving the ion recognition and catalytic performance of these systems. Herein, insights into the cooperativity nature, anion binding strength, and folding mechanism of a model chiral triazole catalyst is presented. Our combined experimental and computational study revealed that multi-interaction catalysts exhibiting weak binding energies (~3-4 kcal mol^{-1}) can effectively recognize ionic substrates and induce chirality, while strong dependencies on the temperature and solvent were quantified. These results are key for the future design of catalysts with optimal anion binding strength and catalytic activity in target reactions.

Introduction

Hydrogen-bond (HB) catalysis represents an important type of activation mode in non-covalent organocatalysis.[1] Alongside the more classical activation of neutral electrophilic substrates, such as carbonyls or nitro derivatives, it has lately also been proved highly effective in reactions involving ionic substrates through the formation of reactive ion-pair intermediates.[2] In particular, it is noteworthy the growing use of this approach in anion-binding catalysis,[2],[3] in which the HB-donor catalyst activates and/or modulates the reactivity of the cationic species of the ionic substrate upon binding to its counteranion. However, despite the remarkable work carried out in the past few years,[2] especially in asymmetric catalysis, the reported methods still present major practical limitations such as high catalyst loadings and long reaction times. These issues have inspired very recent efforts toward the design of more efficient and selective anion-binding catalysts based on multidentate hydrogen-bonding supramolecular structures.[2-4] Among them, macrocyclic bisthiourea or polyamide structures,[4] as well as triazole-based supramolecular catalysts can be highlighted (Figure 1).[5-7]

In particular, triazole HB-donor derivatives have recently attracted great attention due to the several polarized sites present in their scaffolds, which open new opportunities in the interactions that can be involved in the activation step. Thus, since our pioneer application of triazoles as anion-binding catalysts in 2013,[8] several supramolecular triazole-based structures have been designed.[9],[10] The groups of Feringa[6] and Leigh[7] developed molecular rotor and rotaxane catalysts,[11] in which their activity and/or chirality induction efficiency can be switched upon photochemical or protonation reactions (Figure 1A). We proposed a new family of foldamer chiral oligo-triazoles (Figure 1B),[5],[12] which are characterized by having a great modulating capacity and several active sites where the ionic species can be hosted during the reaction process. However, there is a lack of understanding of the binding strength and mechanism of the supramolecular contact ion-pair complex formation in catalysis.[13] Therefore, these interactions lie at the heart of the ion binding catalysis and are of prime interest to understand the mechanism of action. Indeed, a detailed description of the binding

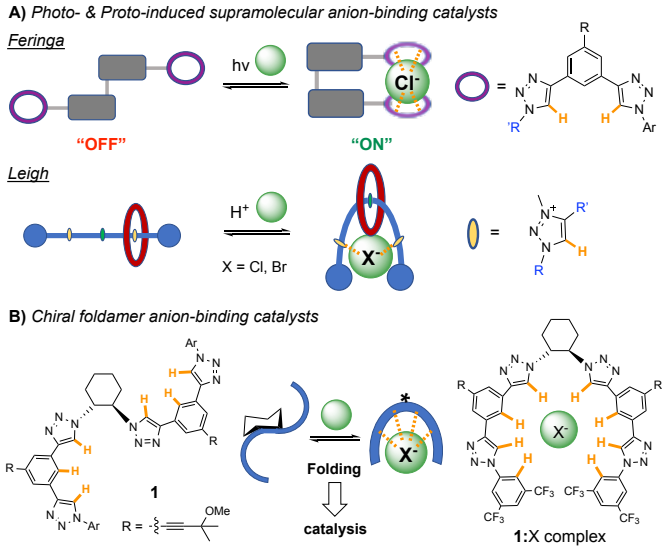

Figure 1. Supramolecular switchable/foldable triazole-based HB-donor anion-binding catalysts.[5-7]

phenomenon with this type of supramolecular structures would be crucial to overcome reactivity and selectivity issues, allowing the prediction of the binding and activity of the host:guest complex, as well as the design of more efficient catalysts. Hence, in this work, we aim at revealing the forces and mechanisms involved in the formation of the supramolecular contact ion pair, as well as bringing some light into the catalytic activity of supramolecular binders.

Results and Discussion

For this study, the chiral TetrakisTriazole **1** (Figure 1B) was chosen as suitable prototypical system. This foldameric catalyst already showed a high activity, presenting one of the lowest catalytic loadings in this field (down to 0.05 mol%), while keeping a high chirality transfer in a series of asymmetric catalytic transformations such as dearomatization reactions of *N*- and *O*-heteroarenes.[5],[14] We began our investigation by exploring the possible dimerization or aggregation of **1** in solution by studying non-linear effects[15] in the model asymmetric Reissert-reaction of quinoline with isopropyl *tert*-butyldimethylsilylketene acetal (Figure 2).[5] Differing from the recent studies with thiourea catalysts that showed an activation/deactivation mechanism,[16] **1** showed close to a 1:1 relationship between the *ee* of the catalyst and the *ee* of the resultant product, which suggests that this type of catalysts stays primarily monomeric during the reaction course.

Next, we examined the binding ability of **1** towards three different types of anions. To this purpose, the non-reactive tetrabutylammonium salts (TBAX) were used as model ionic substrates. The results from ^{1}H NMR titrations and isothermal titration calorimetry (ITC) are summarized in Table 1 (see S.I. for full analysis). Although previous observations suggested a 1:2 or higher order stoichiometry,[14] our present analysis revealed a 1:1 stoichiometry of the catalyst(host):guest complexes for Cl^- and $PhCO_2^-$, while it indicates no binding to TfO^- under these conditions (see Fig. S2 in S.I.).[17] ^{1}H-NMR titration experiments at constant host concentration were then performed at 25 °C using acetone-d_6 as solvent (see Figure 3, right), where a fit with the 1:1 binding model resulted in moderate binding constants for Cl^-

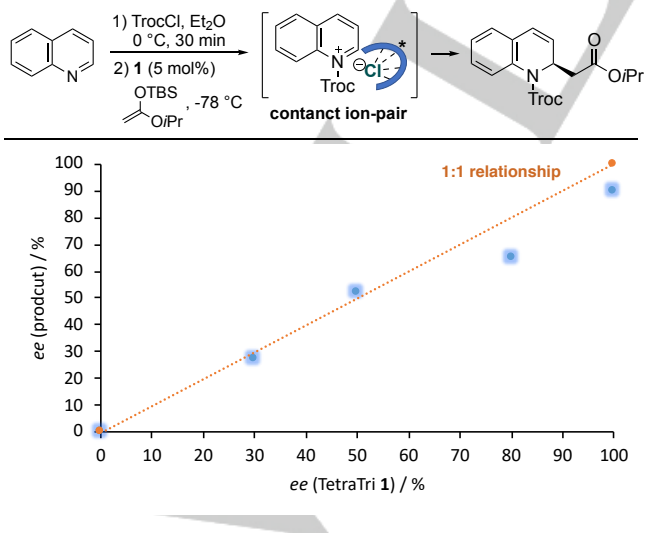

Figure 2. NL-effect study of **1** in the Reissert-reaction of quinoline with a silylketene acetal as nucleophile.

Table 1. Summary of parameters characterizing anion binding of **1** with different TBA salts.

X$^-$	Cl^-	$PhCO_2^-$	TfO^-
Stoichiometry[a]	1:1	1:1	--
^{1}H-NMR, K_a /M^{-1}[b]	536 ± 54	699 ± 56	15 ± 1[e]
ΔG /kcal mol^{-1}[b],[c]	-3.7 ± 0.4	-3.9 ± 0.3	--
ITC, K_a /M^{-1}[d]	305 ± 96	224 ± 90	--
ΔG /kcal mol^{-1}	-3.4 ± 0.2	-2.1 ± 0.6	--
ΔH /kcal mol^{-1}	-1.8 ± 0.5	-3.1 ± 0.3	--
ΔS /cal mol^{-1}	+5.5 ± 0.9	+3.5 ± 2.9	--

[a] Determined through Job Plot analysis (see Fig. S2 in S.I.).[17] [b] NMR-titration of **1** (2 mM) with the corresponding TBAX in acetone-d_6 at 25 °C. K_a fitted using the BindFit software[18] and given as average from two to four measurements. The total fitting error (10 and 8%) is applied to the K_a and ΔG (see S.I. for more details). [c] ΔG derived from K_a (NMR). [d] ITC-titration of 30 mM TBACl into **1** (2 mM) in acetone at 25 °C. [e] Considering a 1:1 complex formation.

(K_a ~ 500 M^{-1}; see Figure 3 and S4) and $PhCO_2^-$ (K_a ~ 700 M^{-1}). Moreover, ITC (Figure 3 and see details in S.I.) provided a Gibbs energy on the order of ΔG ~ -3 kcal mol^{-1} for both weak anion-binding processes, and a small positive entropic contribution (ΔS ~ +5.5 and +3.5 cal mol^{-1} for Cl^- and $PhCO_2^-$, respectively). We note that the low binding constants result in an ITC curve shape deviating from the typical S-shape.[19] This entropy can be explained by the release of solvent molecules from the solvation shell upon binding. Based on the difference between the calculated gas-phase entropies and the measured ΔS, the solvation contribution is ~ +66.5 cal mol^{-1}. However, the most surprising observation was the nearly nonexistent binding to triflate, even though this counter-anion was also proven to be efficient in asymmetric catalysis leading to a highly reactive and enantioselective outcome.[14d] Therefore, it is clear that the standard titration anion-binding analysis is not always appropriate to fully describe and, even more importantly, predict the performance and efficiency of supramolecular binders in catalysis. This can be explained by the different and incompatible conditions used to perform the titration experiments and the reactions. While polar solvents are chosen for titrations to secure homogeneity by complete solubilization of the ionic species, non-polar solvents such as toluene or ethers are required to form the contact ion pair and effect transfer of chirality at low temperatures.

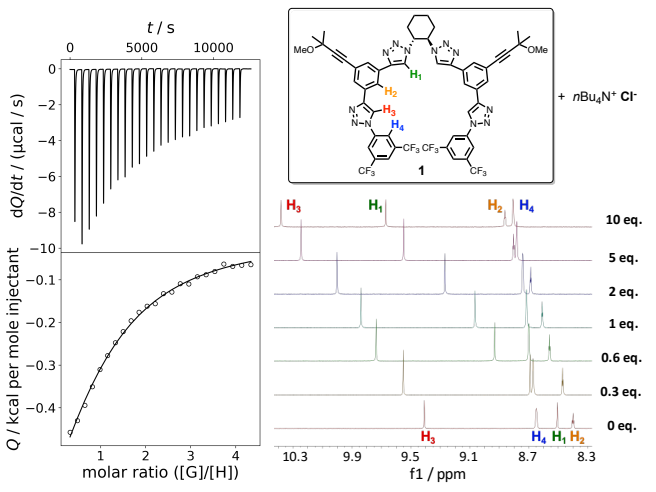

Figure 3. ITC (left) and ^{1}H-NMR titrations (right) of (*R*,*R*)-**1** (2 mM) with TBACl in acetone-d_6.

Taking this into account, we conducted computational studies aiming at providing a detailed description of the non-covalent interactions and delivering key mechanistic insights. For this study, we decided to compare the binding ability of **1** to Cl^- and TfO^- as illustrative counteranions in different solvents and temperatures (Table 2). The most stable structures of the catalyst **1** and its 1:1 and 1:2 host:guest complexes with Me_4NCl and Me_4NOTf as model substrates were first determined at DFT level of theory including zero-point energy correction and the solvent effects of acetone and toluene at 25 °C (titration experiment) and -78 °C (catalytic reaction) (see S.I. for details).[20] Consequently, the binding energies (BE) were computed from the corrected Gibbs energies within the super-molecular approach, defined as: *BE(H:nG)= E(H:nG) – E(H) – nE(G)*. Key solvent and temperature dependencies in the anion recognition were unveiled. For the complexation to Me_4NCl in acetone, a 1:1 stoichiometry is expected based on both the experimental observations and computed BE. Accordingly, the calculated BE of -3.9 kcal mol^{-1} at 25 °C is in very good agreement with the experimentally measured binding energies ΔG of -3.7 kcal mol^{-1} (^{1}H-NMR) and -3.4 kcal mol^{-1} (ITC) (Table1). This weak interaction is strongly reinforced in toluene, especially at -78 °C, giving a prominent interaction of -11.4 kcal mol^{-1} for the 1:1 complex, and showing the possibility of the formation of 1:2 complexes (-14.0 kcal mol^{-1}; ΔBE -2.6 kcal mol^{-1}). Interestingly, though triflate does not appreciably bind in the ^{1}H-NMR titrations (acetone, 25 °C), under the reaction conditions (toluene, -78 °C) the binding and formation of a 1:1 complex can be expected (-3.4 kcal mol^{-1}), explaining the observed performance in catalysis.

Table 2. Calculated BE of the complexes of **1** with Me_4NCl and Me_4NOTf as model substrates.

BE /kcal mol^{-1}	Acetone -78 °C	Acetone 25 °C	Toluene -78 °C	Toluene 25 °C
1:1(Cl)	-4.6	-3.9	-11.4	-8.5
1:2(Cl)	-3.1	-1.1	-14.0	-8.9
1:1(OTf)	3.9	5.6	-3.4	0.0
1:2(OTf)	3.6	7.9	2.2	8.2

We next decided to study in more detail the cooperative interactions involved in the binding process. The entire host:guest (H:G) complex is described by its components, the catalyst (C), anion (A) and substrate (S) (Figure 4, left), and the unit stabilization energy is defined as the sum of all donor and acceptor orbital interactions between a given pair of units of the complex: $E_{unit} = \sum \Delta E_{ij}^{(2)}$, where the stabilization energy is defined as follows (Eq. 1):

$$\Delta E_{ij}^{(2)} = -q_i \frac{|F_{ij}|^2}{\epsilon_j^{(NL)} - \epsilon_i^{(L)}} \qquad (1)$$

with q_i the occupancy of the donor orbital, F_{ij} the off-diagonal Natural Bond Orbital (NBO) Fock matrix element[21] and $\varepsilon_i^{(L)}$,$\varepsilon_j^{(NL)}$ the donor and acceptor orbital energies, respectively. The interactions were evaluated paying special attention to the stabilization energies of the catalyst-anion ($E_{C\text{-}A}$) and catalyst-substrate ($E_{C\text{-}S}$) pairs responsible for the binding, as well as the

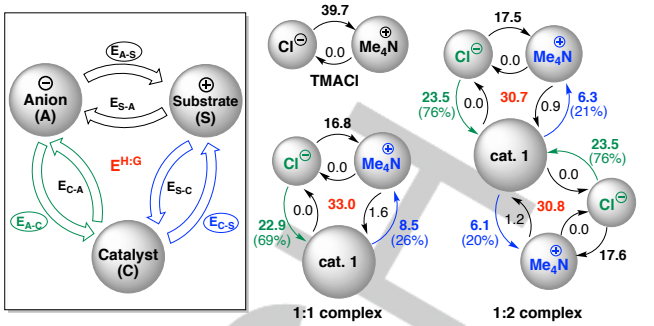

Figure 4. Calculated stabilization energies in kcal mol^{-1} for the most stable 1:1 and 1:2 complexes of **1** with Me_4NCl. Contribution (%) of key interactions to the binding $E^{H:G}$ in brackets.

anion-substrate ($E_{A\text{-}S}$) interaction. The calculated NBO stabilization energies between the units for the 1:1 and 1:2 complexes of **1** with Me_4NCl are given in Figure 4 (see S.I. for more details and complexes with TfO^-). They consider the orbital donor towards the orbital acceptor interactions (shown by the direction of the arrow). In both cases, a notable weakening of the interaction $E_{A\text{-}S}$ of the ammonium salt ion-pair is observed upon binding to the catalyst, i.e. from a strong interaction of 39.7 kcal mol^{-1} to 16.8 and ~17.5 kcal mol^{-1} for the 1:1 and 1:2 complexes, respectively. Moreover, for the 1:1 complex the H:G NBO binding energy ($E^{H:G}$ = $E_{A\text{-}C}$+$E_{C\text{-}A}$+$E_{C\text{-}S}$+$E_{S\text{-}C}$) is 33.0 kcal mol^{-1}, while for the 1:2 complex the stabilization decreases about 2 kcal mol^{-1} for each of the two guest units (Me_4NCl) interacting with the host, showing hence a small destructive interaction of ~4.5 kcal mol^{-1}. However, this does not reflect the ability of the catalyst **1** to recognize the second chloride anion. In fact, the stabilization of the catalyst:chloride anion interaction ($E_{C\text{-}A}$) in the 1:2 complex increases by 7% with respect to the 1:1 complex (from 22.9 to 23.5 kcal mol^{-1}). Though, the interaction between **1** and the substrate Me_4N^+ ($E_{C\text{-}S}$) is being decreased from 26% to ~20% of the total unit stabilization energy.

Next, to monitor the folding towards the **1**:Me_4NCl complex *ab initio* Born Oppenheimer molecular dynamic (BOMD) simulations were run employing DFT-M062X functional and def-SV(P) basis set[22] with the TURBOMOLE package[23] (Figure 5a). We focused on the first steps of the folding process that implies the snapping up of the chloride anion and first catalyst conformational changes to allocate the guest molecule. Despite the weak hydrogen bonding involved, the MD-simulations showed a fast complexation process, which is initiated by the main interaction of the chloride anion with the C-H bonds of the two central triazoles. Next, the opening of one arm of the catalyst takes place in order to leave space for the cationic substrate (Me_4N^+) to enter into the binding cavity, which is driven by additional weak HB-interactions with the nitrogen lone pair (central triazole) of the second arm of the catalyst. The dynamics can be monitored through the changes in the C(cyclohexyl)–N–C(triazole) dihedral angle of the opening arm, which occur within the first 1000 femtoseconds, before it initiates the closing towards the most stable 1:1 complex. Moreover, the CD spectra calculated for the most stable structures could qualitatively reflect both the experimental CD spectral structural signature and the changes in conformation between the non-interacting catalyst **1** and the 1:1 complex (Figure 5b-c and S11).

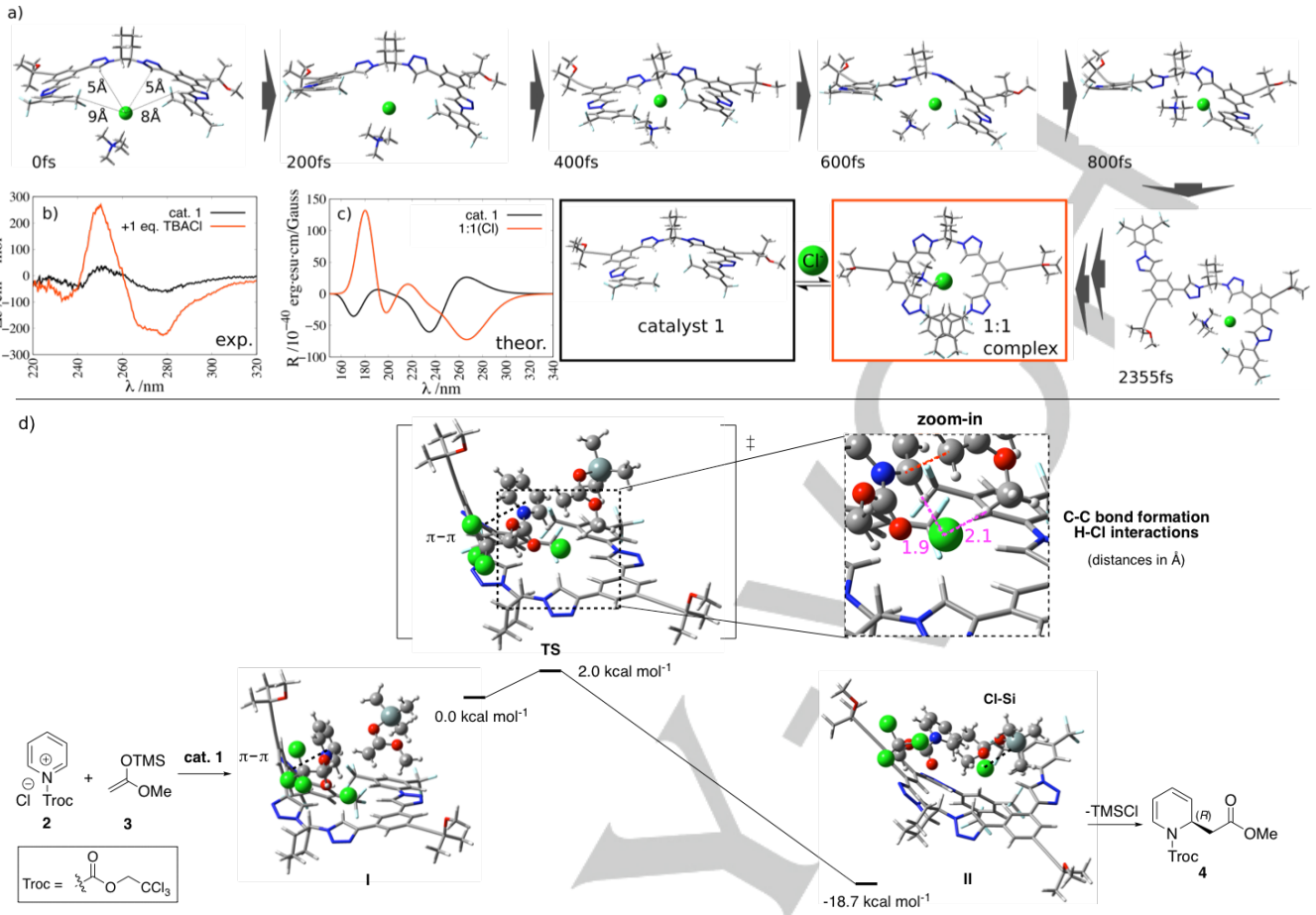

Figure 5. a) Folding mechanism studied by BOMD simulations, b) experimental CD of (*R,R*)-**1** (black line) and after addition of 1 equiv. TBACl (orange line) in THF (62.5 μM), c) calculated CD spectra of **1** (black line) and its 1:1 complex (orange line), and d) computed **TS** for a model Reissert reaction in Et_2O at -78 °C. Zoom-in: new C-C bond (red); C-H-Cl interactions (magenta). See S.I. for details.

Finally, a model enantioselective catalytic Reissert-type reaction employing catalyst (*R,R*)-**1** was investigated computationally. The possible transition state (**TS**) of the reaction of *N*-2,2,2-trichloroethoxycarbonyl (Troc) pyridinium salt **2** as the simplest substrate with silylketene acetal **3** was computed at M06-2X/def2tzvp/ /AM1[24] level of theory in Et_2O at -78 °C (see S.I.), according to the experimental catalytic conditions.[14a] The most plausible kinetically and thermodynamically **TS** is presented in Figure 5d. Similar to the model system, the unit stabilization analysis shows that the ion pair interaction ($E_{A\text{-}S}$) between the pyridinium and the chloride anion in the **TS** is significantly reduced (65% with respect to the weakly bonded complex **I**). Moreover, both pyridinium and nucleophile are stabilized by a HB-interaction with the chloride anion through the C2-H and the MeO-group of **3** with a H-Cl distance of 1.9 and 2.1 Å, respectively. Hence, the nucleophilic attack involves a small barrier of 2.0 kcal mol^{-1}, leading to a more stable intermediate **II** (-18.7 kcal mol^{-1}) that form the final product **4** upon elimination of TMSCl and regeneration of the catalyst **1**. Lastly, the experimentally obtained (*R*)-enantiomer of the product can be explained due to the parallel orientation and weak π–π-interaction between **2** and one arm of **1** in the **TS**, which makes the *Re*-face attack favorable, while the formation of the (*S*)-product is sterically hindered.

Conclusion

To sum up, this study underlines the importance of both the static and dynamic analysis of the anion-binding process for a deeper understanding of the performance of supramolecular receptors in catalysis. Fundamental insight into the competing nature and strength of the anion binding, as well as the recognition and folding mechanism of chiral triazole supramolecular catalysts were unraveled by combining experimental and computational studies. We have learnt that the C-H bonds of the central triazoles are mainly responsible for the initiation of the anion recognition. However, as observed by previous studies with truncated catalysts, the outer triazoles play an important role in attaining high chirality transfer. They present stronger H-bond interactions with the anion than the central triazoles due to their electron poor aromatic substituents, which come closer in the ion-pair complex creating a pseudo-helical structure that can allocate anions with different shapes and sizes. Therefore, the modification at the lower part of the catalyst with different electron deficient groups or by closing the structure into a macrocycle to enforce a quasi-helical structure is expected to lead to more active and efficient chiral anion-binding catalysts. Moreover, calculations on the model reaction showed that the chloride anion in the contact ion-pair complex bridges the cationic substrate and nucleophile via H-bonding. Hence, polarized nucleophiles that can directly interact by HB with different anions within the supramolecular complex provide new opportunities by providing a more rigid hydrogen-bond network, and are currently under investigation in our group.

Acknowledgements

The European Research Council (ERC-CG 724695) and the Deutsche Forschungsgemeinschaft (DFG) within the SFB858 and IRTG2027 are gratefully acknowledged for generous support. We acknowledge the generous allocation of computer time at the high-performance computing PALMA at WWU.

Keywords: Anion-Binding • Supramolecular chemistry • Folding mechanism • Asymmetric organocatalysis • Computational study

[1] A. G. Doyle, E. N. Jacobsen, *Chem. Rev.* **2007**, *107*, 5713-5743.

[2] Selected reviews: a) Z. Zhang, P. Schreiner, *Chem. Soc. Rev.* **2009**, *38*, 1187-1198; b) S. Beckendorf, S. Asmus, O. García Mancheño, *ChemCatChem* **2012**, *4*, 926-936; c) K. Brak, E. N. Jacobsen, *Angew. Chem. Int. Ed*. **2013**, *52*, 534-561; d) M. Mahlau, B. List, *Angew. Chem. Int. Ed*. **2013**, *52*, 518-533.

[3] Pioneer work: a) M. S. Taylor, E. N. Jacobsen, *J. Am. Chem. Soc.* **2004**, *126*, 10558-10559; b) I. T. Raheem, P. S. Thiara, E. A. Peterson, E. N. Jacobsen, *J. Am. Chem. Soc.* **2007**, *129*, 13404-13405. Few selected recent examples: c) A. B. Mayfield, J. B. Metternich, A. H. Trotta, E. N. Jacobsen, *J. Am. Chem. Soc.* **2020**, *142*, 4061-4069; d) D. A. Kutateladze, D. A. Strassfeld, E. N. Jacobsen, *J. Am. Chem. Soc.* **2020**, *142*, 6951-6956; e) Y. Lin, W. J. Hirschi, A. Kunadia, A. Paul, I. Ghiviriga, K. A. Abboud, R. W. Karugu, M. J. Vetticatt, J. S. Hirschi, D. A. Seidel, *J. Am. Chem. Soc.* **2020**, *142*, 5627-5635. For other type of chiral HB-donors: f) A. G. Schafer, J. M. Wieting, T. J. Fisher, A. E. Mattson, *Angew. Chem. Int. Ed.* **2013**, *52*, 11321-11324.

[4] Representative examples: a) Y. Park, K. C. Harper, N. Kuhl, E. E. Kwan, R. Y. Liu, E. N. Jacobsen, *Science* **2017**, *355*, 162-166; b) K. Kang, J. A. Lohrman, S. Nagarajan, L. Chen, P. Deng, X. Shen, K. Fu, W. Feng, D. W. Johnson, L. Yuan, *Org. Lett.* **2019**, *21*, 652-655.

[5] M. Zurro, S. Asmus, S. Beckendorf, C. Mück-Lichtenfeld, O. García Mancheño, *J. Am. Chem. Soc.* **2014**, *136*, 13999-14002.

[6] R. Dorel, B. L. Feringa, *Angew. Chem. Int. Ed.* **2020**, *59*, 785-789.

[7] K. Eichstaedt, J. Jaramillo-Garcia, D. A. Leigh, V. Marcos, S. Pisano, T. A. Singleton, *J. Am. Chem. Soc.* **2017**, *139*, 9376-9381.

[8] S. Beckendorf, S. Asmus, C. Mück-Lichtenfeld, O. García Mancheño, *Chem. Eur. J.* **2013**, *19*, 1581-1585.

[9] a) S. Lee, A. H. Flood, *Binding Anions in Rigid and Reconfigurable Triazole Receptors* In *Click Triazoles* (Ed.: J. Košmrlj). *Topics in Heterocyclic Chemistry*, Springer, Berlin, Heidelberg, 2012, vol. 28, pp 85-107; b) B. Schulze, U. S. Schubert, *Chem. Soc. Rev.* **2014**, *43*, 2522-2571; c) V. Haridas, S. Sahu, P. P. P. Kumar, A. R. Sapala, *RSC Advances*, **2012**, *2*, 12594-12605; d) Y. Hua, A. H. Flood, *Chem. Soc. Rev.* **2010**, *39*, 1262-1271. For additional examples of triazolium and triazole-based anion-binders in catalysis, see e.g.: e) K. Ohmatsu, M. Kiyokawa, T. Ooi, *J. Am. Chem. Soc.* **2011**, *133*, 1307-1309; f) K. Ohmatsu,Y. Ando, T. Ooi, *J. Am. Chem. Soc.* **2013**, *135*, 18706-18709; g) A. Bosmani, S. Pujari, L. Guenée, C. Besnard, A. I. Poblador Bahamonde, J. Lacour, *Chem. Eur. J.* **2017**, *23*, 8678-8684; h) Y. Furukawa, R. Suzuki, T. Nakashima, R. Gramage-Doria, K. Ohmatsu, Takashi Ooi, *Bull. Chem. Soc. Jpn.* **2018**, *91*, 1252-125.

[10] A few selected recent examples of macrocyclic triazole-based anion-binders: a) Y. Liu, W. Zhao, C.-H. Chen, A. H. Flood, *Science* **2019**, *365*, 159-161; b) D. Mungalpara, A. Valkonen, K. Rissanen, S. Kubik, *Chem. Sci.* **2017**, *8*, 6005-6013; c) I.-S. Tamgho, S. Chaudhuri, M. Verderame, D. J. DiScenza, M. Levine, *RSC Adv.* **2017**, *7*, 28489-28493; d) S. Lee, B. E. Hirsch, Y. Liu, J. R. Dobscha, D. W. Burke, S. L. Tait, A. H. Flood, *Chem. Eur. J.* **2016**, *22*, 560-569. See also: e) R. Peng, Y. Xu, Q. Cao, *Chin. Chem. Lett.* **2018**, *29*, 1465-1474.

[11] For other triazole-based anion-binder rotaxanes and catenanes, see e.g.: a) H. Zheng, W. Zhou, J. Lv, X. Yin, Y. Li, H. Liu, Y. Li, *Chem. Eur. J.* **2009**, *15*, 13253-13262; b) Y. Zhao, Y. Li, Y. Li, H. Zheng, X. Yin, H. Liu, *Chem. Commun.* **2010**, *46*, 5698-5700; c) N. G. White, P. D. Beer, *Chem. Commun.* **2012**, *48*, 8499-8501; d) N. G. White, P. D. Beer, *Org. Biomol. Chem.* **2013**, *11*, 1326-1333.

[12] a) S. Hecht, I. Huc, Foldamers: Structure, Properties, and Applications, Wiley-VCH Verlag, 2007, Weinheim. Further selected examples of triazole-based anion-binder foldamers: b) R. M. Meudtner, S. Hecht, *Angew. Chem. Int. Ed.* **2008**, *47*, 4926-4930; c) H. Juwarker, J. M. Lenhardt, D. M. Pham, S. L. Craig, *Angew. Chem. Int. Ed.* **2008**, *47*, 3740-3743; d) Y. Wang, F. Bie, H. Jiang, *Org. Lett.* **2010**, *12*, 3630-3633; e) W. Zhao, Y. Wang, J. Shang, Y. Che, H. Jiang, *Chem. Eur. J.* **2015**, *21*, 7731-7735; f) L. Yang, Y. Wang, Y. Che, H. Jiang, *Org. Biomol. Chem.* **2017**, *15*, 7747-7752; g) D. M. Fidalgo, M. E. Monge, O. Varela, A. A. Kolender, *Eur. J. Org. Chem.* **2018**, 6787-6799; h) Y. Liu, F. C. Parks, W. Zhao, A. H. Flood, *J. Am. Chem. Soc.* **2018**, *140*, 15477-15486; i) F. C. Parks, Y. Liu, S. Debnath, S. R. Stutsman, K. Raghavachari, A. H. Flood, *J. Am. Chem. Soc.* **2018**, *140*, 17711-17723.

[13] a) Y. Liu, A. Sengupta, K. Raghavachari, A. H. Flood, *Chem.* **2017**, *3*, 411-427; b) N. Busschaert, C. Caltagirone, W. Van Rossom, P. A. Gale, *Chem. Rev.* **2015**, *115*, 8038-8155.

[14] a) O. García Mancheño, S. Asmus, M. Zurro, T. Fischer, *Angew. Chem. Int. Ed.* **2015**, *54*, 8823-8827; b) M. Zurro, O. García Mancheño, *Chem. Rec.* **2017**, *17*, 485-498; c) T. Fischer, Q.-N. Duong, O. García Mancheño, *Chem. Eur. J.* **2017**, *23*, 5983-5987; d) T. Fischer, J. Bamberger, M. Gómez-Martínez, D. G. Piekarski, O. García Mancheño, *Angew. Chem. Int. Ed.* **2019**, *58*, 3217-3221.

[15] D. Guillaneux, S.-H. Zhao, O. Samuel, D. Rainford, H. B. Kagan, *J. Am. Chem. Soc.* **1994**, *116*, 9430-9439.

[16] a) D. D. Ford, D. Lehnherr, C. R. Kennedy, E. N. Jacobsen. *J. Am. Chem. Soc.* **2016**, *138*, 7860-7863; b) A. J. Neuvonen, D. Noutsias, F. Topic, K. Rissanen, T. Földes, I. Paṕai, P. M. Pihko, *J. Org. Chem.* **2019**, *84*, 15009-15019.

[17] A predominant 1:1 stoichiometry was concluded from both Job-Plot and computation analysis, the latter providing almost exactly the same binding energies as the ones derived from the NMR titrations using this model. For a discussion of the predictive power of the Job-plot method, see: D. B. Hibbert, P. Thordarson, *Chem. Commun.* **2016**, *52*, 12792-12805.

[18] BindFit v0.5, available at http://app.supramolecular.org/bindfit

[19] W. B. Turnbull, A. H. Daranas, *J. Am. Chem. Soc.* **2003**, *125*, 14859-14866.

[20] The optimizations were carried out in the gas phase at DFT-M06-2X/6-31G(d,p) level [a) Y. Zhao, D. G. Truhlar, *Theor. Chem. Acc.* **2008**, *120*, 215-241] with the Gaussian16 program [b) M. J. Frisch, *et al*. Gaussian16 Revision B.01. 2016; Gaussian Inc. Wallingford CT]. The solvation energies were calculated with COSMOtherm [Version C3.0; COSMOlogic GmbH and Co. KG, http://www.cosmologic.de; c) A. Klamt, *J. Phys. Chem.* **1995**, *99*, 2224-2235] at BP86/TZVP level of theory [d) J. P. Perdew, *Phys. Rev. B* **1986**, *33*, 8822-8824]. Additional quasi-rigid-rotor-harmonic oscillator for erroneous entropic behavior, counter-poise (CP) correction for electronic energies to minimize the basis set superposition error arising from the relatively small basis set used for the optimization search, as well as the amount-of-substance fraction according to the Boltzmann distribution were included (see S.I. for details).

[21] a) J. P. Foster, F. Weinhold, *J. Am. Chem. Soc.* **1980**, *102*, 7211-7218; b) E. D. Glendening, A. E. Reed, J. E. Carpenter, F. Weinhold, NBO Version 3.1.

[22] A. Schäfer, H. Horn, R. Ahlrichs, *J. Chem. Phys.* **1992**, *97*, 2571-2577.

[23] TURBOMOLE V7.3 2019, TURBOMOLE GmbH; available from http://www.turbomole.com

[24] a) F. Weigend, R. Ahlrichs, *Phys. Chem. Chem. Phys.* **2005**, *7*, 3297-3305; b) M. J. S. Dewar, E. G. Zoebisch, E. F. Healy, J. J. P. Stewart, *J. Am. Chem. Soc.* **1985**, *107*, 3902-3909.

Entry for the Table of Contents

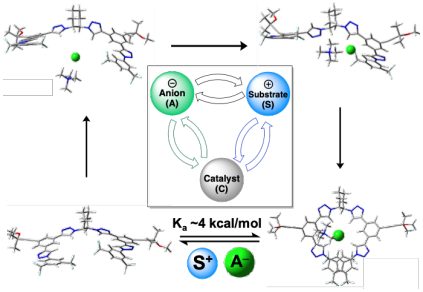

Brought into the fold! Fundamental insight into the folding mechanism, cooperativity nature and anion binding strength requirements in supramolecular anion-binding catalysis is presented. This is afforded by a combined experimental and computational study with a prototypical foldameric triazole-based chiral anion-binding catalytic system, implying multi-recognition sites to the ionic substrate units and weak binding energies as success factors.